

Fines content influence on the dynamic slope behavior in small-scale physical models

Vedran Jagodnik^{(1,2)*}, Davor Marušić⁽¹⁾, Željko Arbanas⁽¹⁾, Nina Čeh⁽¹⁾, Josip Peranić⁽¹⁾, Martina Vivoda Prodan⁽¹⁾

1) University of Rijeka, Faculty of Civil Engineering, Radmile Matejčić 3, Rijeka, Croatia, +38551265941
(vedran.jagodnik@gradri.uniri.hr)

2) Center for Artificial Intelligence and Cybersecurity, University of Rijeka, Radmile Matejčić 2, Rijeka, Croatia

Abstract Small-scale physical models have already been used for some time to simulate the natural slope behaviour subjected to static and dynamic loading. This research presents the results of small-scale physical slope models with a 40° slope inclination that were made by using pure sand specimens and two artificial mixtures of sand and kaolinite powder with different mass ratios. Physical models were saturated and subjected to dynamic loading to simulate the behaviour of slopes that can form shallow landslides. The shaking table was used to apply the dynamic loading, using a loading frequency of 5.5 Hz and a horizontal displacement amplitude of 0.2 cm. Using two high-speed cameras, the model's surface displacements were measured. Accelerometers were placed inside the slope body to measure the acceleration response during dynamic loading. Performed simulations showed the significance of fines content on the dynamic slope behaviour. Unlike the models made with pure sand, slopes with mixtures of sand and kaolinite powder were able to withstand a larger number of loading cycles without any amplification recorded during cyclic loading. The crown and the foot of the slope have proven to be the most critical parts in small-scale models. The presented results are focused on the loading time necessary for the first crack to open on a small-scale slope model. Cracks on the slope's surface formed during the dynamic loading can infiltrate additional water, ensuring locally higher slope saturation resulting in soil softening and additional strength degradation. The influence of fines content on the response of the small-scale slope model was presented simply by comparing the time of the crack appearance. The results show that the slope made from pure sand was the most critical one out of three tested materials.

Keywords landslide, small-scale model, dynamic soil behaviour, sand-clay mixtures

Introduction

Two primary factors responsible for the initiation of landslides are precipitation and seismic activity. If heavy rainfall is closely followed by an earthquake, a catastrophic event may occur (e.g., Popescu 2002; Chen et al. 2012; Wu et al. 2015). The seismic shaking induces shear strain in the

soil, resulting in the degradation of its structural integrity and subsequent collapse. Slopes that are susceptible to shallow landslides are particularly influenced by both earthquakes and rainfall (Gabet and Mudd 2006; Yang and Luo 2015). As defined by the ICL (Icl 2016), shallow landslides are typically characterized by a depth of approximately five meters.

Both basic and sophisticated physical models were studied to better understand the process and behaviour of slopes. For the past thirty years, researchers have focused on the initiation, accumulation, and mechanism of landslides that are caused by water seeping into a slope (Spence and Guymer 1997; Wang and Sassa 2001; Okura et al. 2002; Rahardjo et al. 2002; Kim et al. 2004; Moriwaki et al. 2004; Ochiai et al. 2004; Orense et al. 2004; Pajalić et al. 2021). Additionally, research is carried out on small-scale models under dynamic loads (Ichii and Ohmi 2004; Cao et al. 2019) with a focus on examining the slope behaviour under different dynamic loading scenarios.

Landslide modelling requires the application of similarity laws to accurately simulate the behaviour of landslides. These laws ensure that the model experiments represent the prototype conditions as accurately as possible. The similarity laws include geometric, kinematic and dynamic similarity simultaneously (You et al. 2012; Lai et al. 2013; Pajalić 2024). The complexity of the similarity laws can be depicted in Figure 1. In the case of earthquake-induced landslides, seismic parameters, topography and landform features, and engineering properties of soil are considered the main factors affecting landslide dynamics (Stark and Hovius 2001). The choice of similar materials and mix proportions is also important in landslide model tests (Baronin 1992).

The scaling principles for modelling a large-scale prototype subjected to an earthquake were described simply by Iai et al. in 2005. The shear modulus at small deformation ($\leq 10^{-6}$) is assumed to be proportional to the square root of confining pressure. This results in Type II relations, which are frequently applied to models that employ sand that is identically dense like the material in the prototype (Iai et al. 2005).

The relationship between dynamic loads and other potential mechanisms leading to failure can be defined and described using the dynamic characteristics of soil. An

earthquake causes cyclic loading of the soil. Different amplitudes and frequency of cyclic shear stresses are applied to the soil, which can cause both temporary and permanent deformations (Pecker 2008).

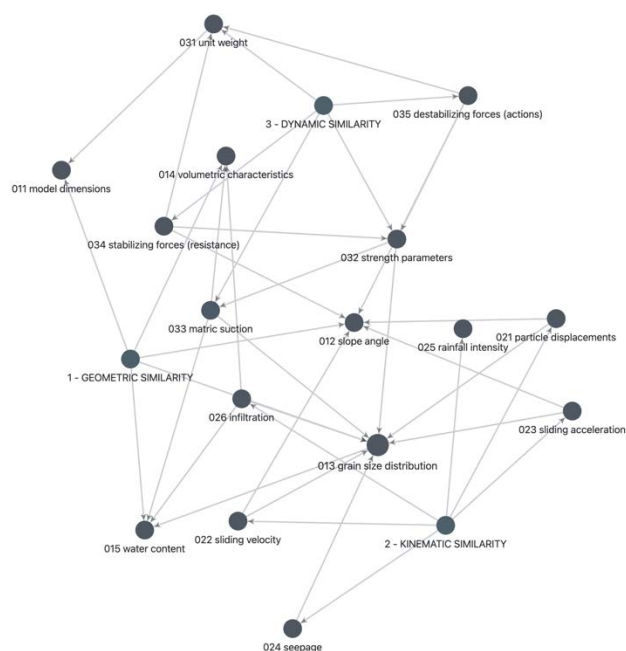


Figure 1 Complexity of similarity law interactions

The results in this paper are the outcome of a four-year research project titled “Physical modelling of landslide remediation constructions behaviour under static and seismic actions” that was funded by the Croatian National Science Foundation. An example of a small-scale slope made from different material is examined on the dynamic loading. A scaling factor of 40 was applied following the property scaling defined by (Iai et al. 2005). The motivation behind this research was to examine the mechanics of shallow landslides in a small-scale model under dynamic excitation and to examine the influence of remediation measures on the small-scale slope behaviour under dynamic excitation.

Methodology

Model setup

The tests were performed in fine-grained sand called Drava sand (0–1.0 mm) and the mixtures of Drava sand and kaolin powder in 10% and 15% mass ratio. Material made purely out of Drava sand has been assigned with the ID “SK0”, while the material with 10% and 15% of kaolin powder have been assigned with the IDs’ “SK10” and “SK15”, respectively. The grain size distribution of sand used is presented in Figure 2. The physical properties of the selected materials are presented with Tab. 1. The small-scale slope model was scaled according to the scaling laws defined by Iai et al. 2005). In this case, scaling factors for 1g conditions were used and summarised in Tab.

2. The width of the model box is 50 cm. The length of the model is around 90cm. The slope angle, which was constant throughout all three tests, was 40°. This assured the critical acceleration to be smaller than the slope angle.

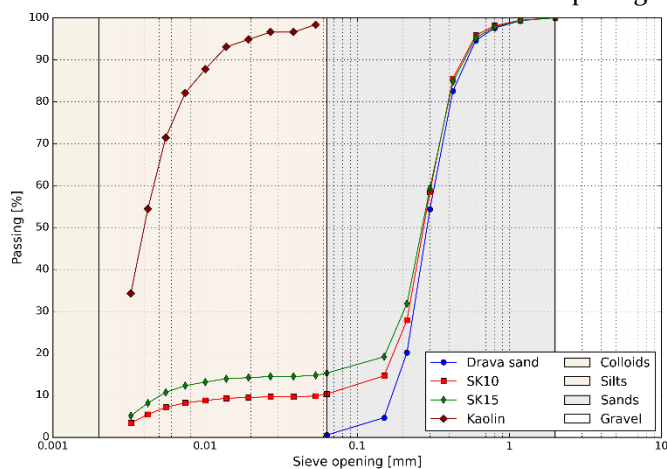


Figure 2 Sieve analysis of basic material and its mixtures

Table 1 Physical properties of testing materials

Physical property	Symbol	SK0	SK10	SK15
Specific gravity	G_s [-]	2.7	2.69	2.67
Particle size	D_{10} [mm]	0.183	0.054	0.0045
	D_{30} [mm]	0.237	0.219	0.206
	D_{60} [mm]	0.32	0.307	0.303
Coefficient of uniformity	C_u [-]	1.749	5.685	-
Coefficient of curvature	C_c [-]	0.959	2.893	-
Minimum void ratio	e_{min} [-]	0.641	0.647	0.544
Maximum void ratio	e_{max} [-]	0.911	1.121	1.43
Initial relative density	$D_{r,i}$ [%]	50	50	75

Table 2 Scaled properties based on the similarity laws

Property	Scaling factor, Type II	Value
Length	μ	40
Time	$\mu^{0.75}$	15.91
Frequency	$\mu^{-0.75}$	0.0635
Stress	$\mu^{0.5}$	6.32
Displacement	$\mu^{1.5}$	252.98
Acceleration	1	1

Material was built in a small-scale frame made of aluminium and plexiglass applying the undercompaction method proposed by Ladd (1978). The height of each layer was calculated based on the considered layer undercompaction, as stated in the equation (1).

$$U_n = U_{n,i} - \left[\frac{(U_{n,i} - U_{n,t})}{n_t - 1} \cdot (n - 1) \right] \quad [1]$$

where: U_n is an undercompaction of a layer being considered, $U(n,i)$ is the chosen value of percent of undercompaction of the first layer, n is the number of layer being considered and n_t is the total number of layers.

Measuring equipment

Several different measuring techniques were used and applied. Two governing measuring equipment were: (i) surface marker points for monitoring the displacement using a pair of high-speed cameras and (ii) accelerometers. The type of accelerometers used are presented in Figure 3. The Seika BDK₃ accelerometer is an analogue measuring instrument designed to measure acceleration within a range of $\pm 3g$. It operates within a frequency range of 1 to 300 Hz, and its sensitivity is 150 mg/V when subjected to a 5V excitation. The position of accelerometers inside the model itself is presented in Figure 4.

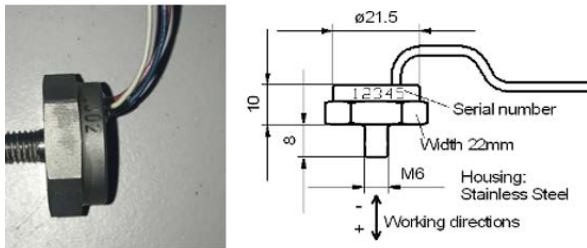


Figure 3 Seika BDK₃ accelerometer used for monitoring accelerations inside small-scale model

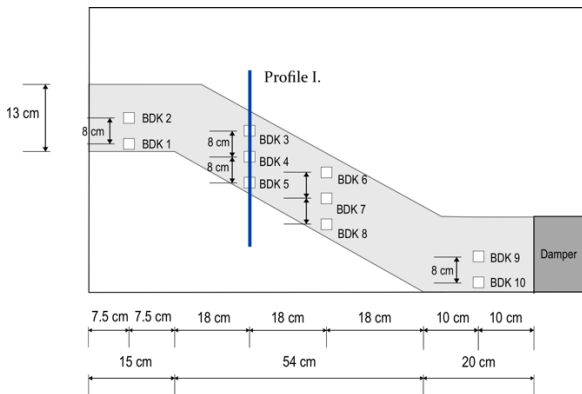


Figure 4 Positions of the measuring equipment inside the small-scale slope model

GOM Aramis 4M system of high-speed cameras is used, with each camera’s resolution of 2400x1728 pixels. Each measurement is conducted with 100 fps and post-processed using digital image correlation.

Shake table system

The Quanser STI-III seismic platform is a versatile biaxial shake table system, with 120 kg mass capacity. It can reproduce ground motions to examine shaking responses of subjected materials and/or constructions. With a travel range of ± 10.8 cm in both the x and y directions, this

system allows for comprehensive testing under various seismic scenarios. Its operational bandwidth is 10 Hz, making it a reliable tool for earthquake engineering research. The biaxial design enhances its capability to replicate complex seismic motions, providing valuable insights into the performance of subjected structures in multidirectional forces. Figure 5 presents the small-scale slope model positioned on the shaking table.

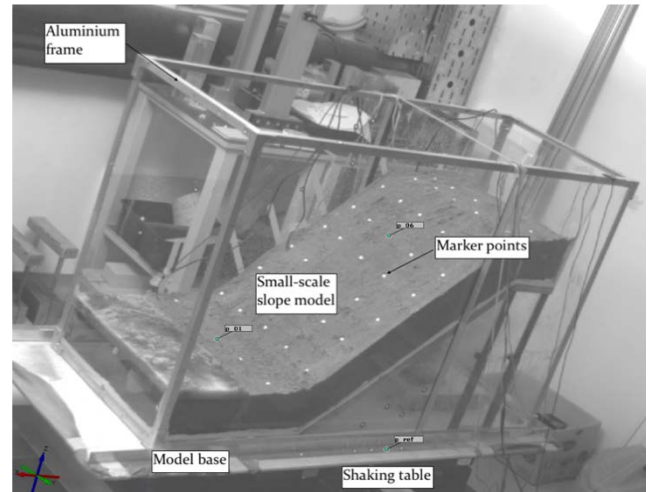


Figure 5 High-speed camera photo before the test initiation

Results

The results of dynamic test on small-scale models made from different types of material are presented in the following section. Acceleration measured using Seika BDK₃ accelerometers in combination with high-speed cameras were used to determine the time needed for first crack to appear during dynamic loading.

Model slopes are loaded with sinusoidal dynamic loading like the one presented on Figure 6. The amplitude of dynamic loading was 0.2cm and the frequency was gradually increased from 0Hz to 5.5Hz in 10 seconds, and decreased in the last 10 seconds. The loading lasted for 60 seconds.

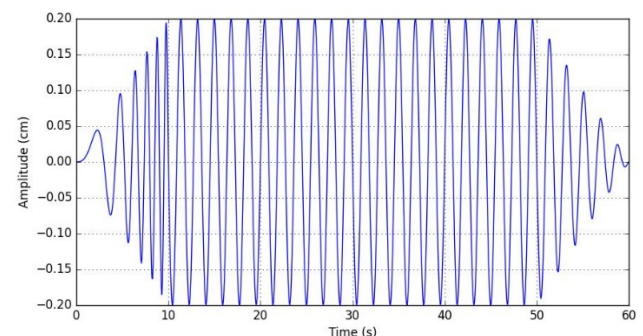


Figure 6 The shape of dynamic loading applied with shaking table

The time of the first crack appearance is marked with the dashed red line, as presented in Figure 7.

Results of a dynamic test on pure sand (SK0)

A small-scale slope model made of pure sand withstood a load of about 35 seconds before the first crack appeared. The acceleration plots of the BDK3 and BDK4 accelerometers placed inside the model are shown in Figure 7(a). The maximum acceleration measured by the BDK3 accelerometer (Figure 4) at the top of the slope model is 0.25g.

Results of a dynamic test on sand mixed with 10% of kaolin (SK10)

The acceleration plots of the BDK3 and BDK4 accelerometers placed in a small-scale slope model made of sand mixed with 10% kaolin are shown in Figure 7(b). The model withstood approximately 55 seconds of loading before the first crack appeared. Figure 7(b) shows that the

accelerations decrease again after about 65 seconds of testing. This time corresponds to a further opening of the tension crack, which occurred for the first time in the 55th second of a test. The maximum acceleration measured with the accelerometer BDK3 (Figure 4) at the top of the slope model is 0.35 g.

Results of a dynamic test on sand mixed with 15% of kaolin (SK15)

The physical model of a small-scale slope model made of sand mixed with 15% kaolin has shown that it can withstand a dynamic load of about 40 seconds. At $t=40s$ the first crack appeared. The acceleration diagrams of BDK3 and BDK4 are shown in Figure 7(c). The maximum acceleration measured by the accelerometer BDK3 (Figure 4) at the top of the slope model is 0.45g.

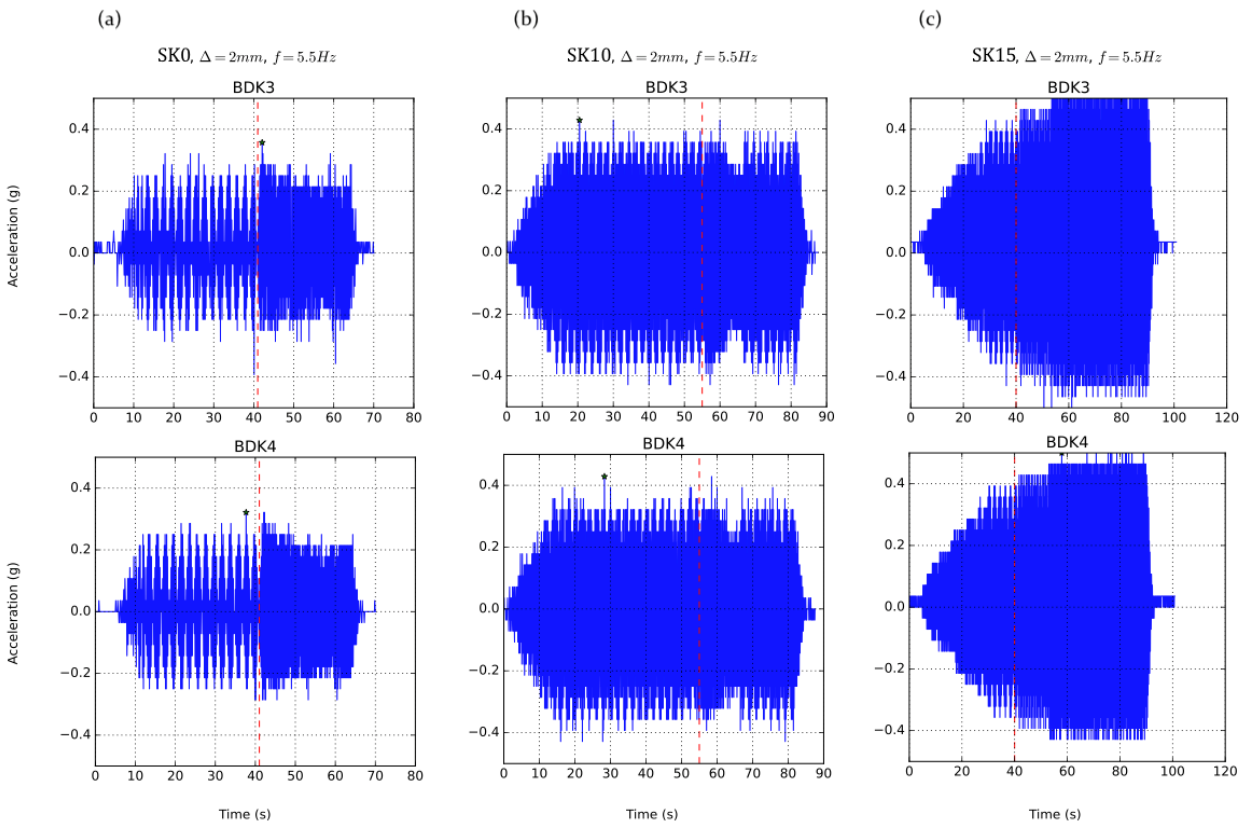


Figure 7 Accelerations of small-scale model made from pure sand

Analysis of performed test

Based on the results of dynamic test on a small-scaled slopes made from different materials, time necessary for a first crack to appear was detected. The values are summarised in Tab 3. The recorded times are normalized with respect to the time corresponding with the results of a model made form pure sand ($t_{crack,SK0} = 35s$) using the equation (2):

$$T_N = \frac{t_{crack,ID}}{t_{crack,SK0}} \quad [2]$$

The plot of normalized time failure and percent of fines are presented with the Figure 8.

Table 3 Scaled properties based on the similarity laws

Model material, ID	Time of first crack, $t_{crack,ID}$ (s)	% of material <63 μ m	% of material <2 μ m	Normalized time of first crack, T_N (-)
Pure sand (SK0)	35	<1	0	1.00
Sand with 10% of kaolin (SK10)	55	10	≈3.5	1.57
Sand with 15% of kaolin (SK15)	40	15	≈5	1.14

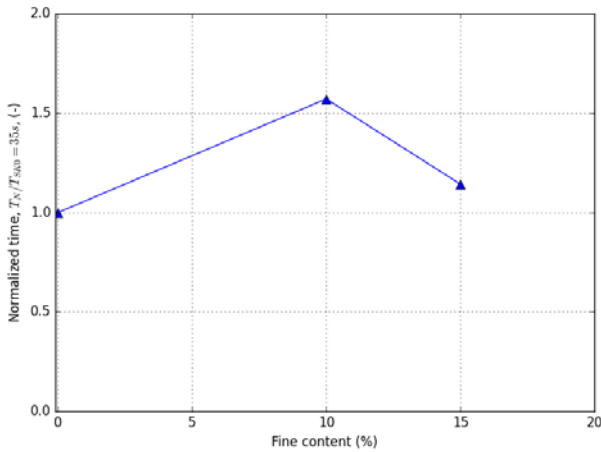


Figure 8 Normalized time failure with respect to fines content

Discussion

The influence of fines content on cyclic soil behaviour can simply be characterised with the cyclic shear strain threshold for pore water pressure generation, degradation, etc. (Vucetic 1994; Mortezaie and Vucetic 2016; Ichii and Mikami 2018). This is consistent if the response of materials with the ID’s “SKo” and “SK1o” are compared. Since mixture “SK1o” has a plasticity index, the cyclic threshold is larger than in ”SKo”. This led to the time of the first crack appearance 36% greater than for slope made of “SKo”. By further increasing the fines content, the plastic index should be larger, thus the threshold should be larger for “SK15” compared to “SK1o”, making the material subjectable to a larger number of cycles. If the times of first crack appearance in “SKo” and “SK15” are compared, the material “SK15” can be subjected to dynamic loading for 12% longer. But, if the materials “SK1o” and “SK15” are compared, “SK15” can be subjected to dynamic loading 27% less. This is due to inter-grain connections and the formation of metastable soil, in combination with the presence of low confining pressure.

Conclusions

In conclusion, this comprehensive study provides valuable insights into critical small-scale slope behaviour, subjected to dynamic loading. The inter-grain connections and interactions emerge as a significant element, influencing the overall performance of the soil matrix. Significantly, the identification of pore water pressure thresholds and fines content thresholds contributes to the understanding

of small-scale slope behaviour. The role of overburden stress under ig conditions significantly impacts soil behaviour, from which slope models were made. Further analysis will be made to examine the inter-grain interaction and behaviour at low confining stresses under static and dynamic loading for both artificial and natural soil mixtures.

Acknowledgements

Physical modelling of landslide remediation constructions behaviour under static and seismic actions (ModLandRemSS, IP-2018-01-1503) funded by Croatian Science Foundation
 “Laboratory Research of Static and Cyclic Behavior at Landslide Activation” (uniri-tehnic-18-113) funded by the University of Rijeka, Croatia

References

Baronin V V. (1992) Modeling of landslide-generated surges. *Hydrotechnical Construction* 26:280–285. <https://doi.org/10.1007/BF01545039>

Cao L, Zhang J, Wang Z, et al (2019) Dynamic response and dynamic failure mode of the slope subjected to earthquake and rainfall. *Landslides* 16:1467–1482. <https://doi.org/10.1007/s10346-019-01179-7>

Chen XL, Zhou Q, Ran H, Dong R (2012) Earthquake-triggered landslides in southwest China. *Natural Hazards and Earth System Sciences* 12:351–363. <https://doi.org/10.5194/nhess-12-351-2012>

Gabet EJ, Mudd SM (2006) The mobilization of debris flows from shallow landslides. *Geomorphology* 74:207–218. <https://doi.org/10.1016/j.geomorph.2005.08.013>

Iai S, Tobita T, Nakahara T (2005) Generalised scaling relations for dynamic centrifuge tests. *Geotechnique* 55:355–362. <https://doi.org/10.1680/geot.2005.55.5.355>

Ichii K, Ohmi H (2004) Slope stability of cohesionless material under large seismic shakings. In: 11th international conference on soil dynamics and earthquake engineering and the 3rd international conference on earthquake geotechnical engineering proceedings. pp 388–395

Icl (2016) Instruction for World Reports on Landslides

Kim J, Jeong S, Park S, Sharma J (2004) Influence of rainfall-induced wetting on the stability of slopes in weathered soils. *Eng Geol* 75:251–262. <https://doi.org/https://doi.org/10.1016/j.enggeo.2004.06.017>

Ladd R (1978) Preparing Test Specimens Using Undercompaction. *Geotechnical Testing Journal* 1:16–23. <https://doi.org/10.1520/GTJ10364J>

Lai CJ, Zhu YP, Wang CQ, Ma TZ (2013) Theory Study on Similitude Design of Shaking Table Tests of Earthquake-Induced Landslide. *Applied Mechanics and Materials* 353–356:2294–2300. <https://doi.org/10.4028/www.scientific.net/AMM.353-356.2294>

- Moriwaki H, Inokuchi T, Hattanji T, et al (2004) Failure processes in a full-scale landslide experiment using a rainfall simulator. *Landslides* 1:277–288. <https://doi.org/10.1007/s10346-004-0034-0>
- Ochiai H, Okada Y, Furuya G, et al (2004) A fluidized landslide on a natural slope by artificial rainfall. *Landslides* 1:211–219. <https://doi.org/10.1007/s10346-004-0030-4>
- Okura Y, Kitahara H, Ochiai H, et al (2002) Landslide fluidization process by flume experiments. *Eng Geol* 66:65–78. [https://doi.org/10.1016/s0013-7952\(02\)00032-7](https://doi.org/10.1016/s0013-7952(02)00032-7)
- Orense RP, Shimoma S, Maeda K, Towhata I (2004) Instrumented Model Slope Failure due to Water Seepage. *Journal of Natural Disaster Science* 26:15–26. <https://doi.org/10.2328/jnds.26.15>
- Pajalić S (2024) Contribution to the development of similarity laws in small-scale landslide physical models (in preparation). PhD Thesis, University of Rijeka, Faculty of Civil Engineering
- Pajalić S, Peranić J, Maksimović S, et al (2021) Monitoring and data analysis in small-scale landslide physical model. *Applied Sciences (Switzerland)* 11:. <https://doi.org/10.3390/app11115040>
- Pecker A (2008) Advanced earthquake engineering analysis. In: CISM International Centre for Mechanical Sciences, Courses and Lectures. SpringerWienNewYork, pp 1–13
- Popescu ME (2002) Landslide causal factors and landslide remedial options. In: 3rd International Conference on Landslides, Slope Stability and Safety of Infra-Structures. pp 61–81
- Rahardjo H, Leong EC, Rezaur RB (2002) Studies of rainfall-induced slope failures. pp 15–29
- Spence KJ, Guymer I (1997) Small-scale laboratory flowslides. *Géotechnique* 47:915–932. <https://doi.org/10.1680/geot.1997.47.5.915>
- Stark CP, Hovius N (2001) The characterization of landslide size distributions. *Geophys Res Lett* 28:1091–1094. <https://doi.org/10.1029/2000GL008527>
- Wang G, Sassa K (2001) Factors affecting rainfall-induced flowslides in laboratory flume tests. *Géotechnique* 51:587–599. <https://doi.org/10.1680/geot.2001.51.7.587>
- Wu LZ, Huang RQ, Xu Q, et al (2015) Analysis of physical testing of rainfall-induced soil slope failures. *Environ Earth Sci* 73:8519–8531. <https://doi.org/10.1007/s12665-014-4009-8>
- Yang J, Luo XD (2015) Exploring the relationship between critical state and particle shape for granular materials. *J Mech Phys Solids* 84:196–213. <https://doi.org/10.1016/j.jmps.2015.08.001>
- You Y, Liu J, Chen X (2012) Study on Similarity Laws of Model Experiments of Debris Flow Channels. In: 2012 2nd International Conference on Remote Sensing, Environment and Transportation Engineering. IEEE, pp 1–5